Theory of defects in conducting polymers. I. Theoretical principles and simple applications

1991 J. Phys.: Condens. Matter 3 3879

(http://iopscience.iop.org/0953-8984/3/22/002)

J. Phys.: Condens. Matter 3 (1991) 3879–3903. Printed in the UK

Theory of defects in conducting polymers: I. Theoretical principles and simple applications

D S Wallace†‡¶, A M Stoneham§, W Hayes†, A J Fisher†‡ and A H Harker‡

† Clarendon Laboratory, Parks Road, Oxford OX1 3PU, UK
‡ Theoretical Physics Division, Harwell Laboratory, Oxon OX11 0RA, UK
§ AEA Industrial Technology, Harwell Laboratory, Oxon OX11 0RA, UK

Received 14 November 1990, in final form 12 February 1991

Abstract. We describe a method for solving simultaneously the Hartree–Fock equations of motion in the zero differential overlap approximation for the electronic structure of a molecule and the dynamical equations of motion for its atoms. Our approach is similar to that of Car and Parrinello in that we optimize the electronic structure and the geometry simultaneously, but differs in that we make a chosen number of iterations towards electronic self-consistency at each geometry rather than treating the electron wavefunctions as dynamical variables. We give examples of the use of the method to calculate the equilibrium geometries, dipole moments, molecular polarizabilities and vibrational frequencies of small molecules. In the following paper we apply this approach to problems of defect processes in conducting polymers.

1. Introduction

For many years the standard approach to optimizing the geometry of a molecular system was to fix the atomic positions, calculate the electronic structure using one of the many methods of varying sophistication that are available and then relax the geometry in response to forces calculated either directly from the electronic structure and the core–core repulsion or by numerical differentiation of the total energy. Whilst other approaches were from time to time exploited for one-electron defect systems in solids (e.g. Stoneham and Bartram 1970), the same strategy was also standard in defect studies. Recently, however, following the work of Car and Parrinello (1985) there has been great interest in methods that treat the optimization of electronic structure and of geometry as a single problem and perform them simultaneously.

The original Car–Parrinello method involves solving the electronic part of the problem using the local density approximation to density functional theory. The method incorporates a basis set of plane waves for the electrons with norm-conserving pseudopotentials and finds the global minimum of the energy function for the whole system using damped molecular dynamics. The electron wavefunctions are assigned a fictitious mass and treated as classical dynamical variables on the same footing as the atomic positions; the resulting system is then allowed to evolve with time according to

¶ Present address: Andersen Consulting, 2 Arundel Street, London WC2R 3LT, UK.

0953-8984/91/223879+25$03.50

the Euler–Lagrange equations of motion, subject to the constraint that the wavefunctions remain orthonormal. The minimum-energy configuration is found by simulated quenching or annealing of these dynamics; alternatively, if no quenching is performed, the method yields genuine information about the dynamics of the system. These techniques have been applied with great success to simulations of crystalline silicon (Car and Parrinello 1985), amorphous silicon (Car and Parrinello 1988), amorphous carbon (Galli *et al* 1989), grain boundaries in germanium (Payne et al 1987, Tarnow et al 1989) and the germanium (100) surface (Needels *et al* 1987). A slightly different approach has been advocated by Gillan (1989) and applied to a calculation of the formation energy of the aluminium vacancy; it retains the fundamental Car–Parrinello principle of calculating the electronic structure and the geometry simultaneously, but sacrifices information about the atomic dynamics in favour of a more efficient algorithm, based on the conjugate-gradient method, for finding the overall minimum in the energy function; the electronic part of the energy functional is still obtained from the local density approximation with a plane-wave basis.

In the work described in this and the following paper, we seek to apply the principles of the above methods to many of the much more complicated problems in physics and chemistry which involve both electronic excitation and structural distortion of molecules. This is out of the question with *ab initio* methods of electronic structure, since the calculations listed above already strain present-day computers to the limit; rather, we seek to replace the local density approximation by the semi-empirical approximations of quantum chemistry (Pople and Beveridge 1970), which have been tested on a wide variety of molecules over many years and whose successes and limitations are well known. Because we wish to retain information about the dynamics of the system we use the molecular-dynamics method with simulated annealing for the atomic motion. However, we find that, with the minimal basis sets used in the semi-empirical zero-differential-overlap methods, the advantages of using molecular dynamics to relax the electronic wavefunctions disappear. In the next section we introduce the semi-empirical approach to electronic structure and derive expressions for the forces experienced by the atoms during the dynamical process. We then discuss the difficulties inherent in enforcing the orthogonality constraint if the wavefunctions are made to relax by following dynamical equations of motion and explain why we have not adopted this approach. Finally we explain the capabilities of the method as we have implemented it and give examples of its use to calculate a number of properties of small molecules.

2. Introduction to semi-emprical approximations

The two basic approximations of Hartree–Fock theory are the Born–Oppenheimer approximation and the assumption that the overall electronic wavefunction can be written in terms of a single Slater determinant of one-electron wavefunctions. These one-electron functions are usually made up of a linear combination of atomic orbitals, often either Gaussian orbitals of some form or Slater-type orbitals (STO). The latter are used here. In zero external magnetic field it can be assumed, without loss of generality, that both the basis orbitals and the expansion coefficients are real. By expressing the wavefunctions in LCAO terms as:

$$\psi_i^\sigma = \sum_\nu c_{\nu i}^\sigma \phi_\nu \tag{1}$$

where σ is a spin label and the Schrödinger equation is replaced by a pair of matrix equations, where the elements of the matrices are the molecular orbital expansion coefficients. We follow standard practice in labelling atomic orbitals with Greek suffixes and molecular orbitals with Roman ones. These matrix equations (the Hartree–Fock–Roothaan or HFR equations) are:

$$\sum_{\nu}(F^{\sigma}_{\mu\nu} - \lambda^{\sigma}_{i} S_{\mu\nu})c^{\sigma}_{\nu i} = 0$$

or

$$\mathbf{F}^{\sigma}\mathbf{c}^{\sigma} = \mathbf{S}\mathbf{c}^{\sigma}\lambda^{\sigma}. \tag{2}$$

Here λ^{σ} is the (diagonal) matrix of one-electron energies for spin σ, $\mathbf{S}$ is the overlap matrix and $\mathbf{F}^{\sigma}$ is the Fock matrix for spin σ, given by

$$F^{\sigma}_{\mu\nu} = H_{\mu\nu} + \sum_{\lambda\rho}\left[P_{\lambda\rho}(\mu\nu|\lambda\rho) - P^{\sigma}_{\lambda\rho}(\mu\rho|\lambda\nu)\right]. \tag{3}$$

$\mathbf{H}$ is the one-electron Hamitonian matrix and $\mathbf{P}^{\sigma}$ is the bond-order matrix for spin σ defined in turn by

$$P^{\sigma}_{\lambda\rho} = \sum_{i}^{\text{occupied}} c^{\sigma}_{\lambda i}c^{\sigma}_{\rho i}$$
$$P_{\lambda\rho} = P^{\sigma}_{\lambda\rho} + P^{-\sigma}_{\lambda\rho} \tag{4}$$

and

$$(\mu\nu|\lambda\rho) = \int \mathrm{d}^3\mathbf{r}_1 \int \mathrm{d}^3\mathbf{r}_2\, \phi_{\mu}(\mathbf{r}_1)\phi_{\nu}(\mathbf{r}_2)|\mathbf{r}_1 - \mathbf{r}_2|^{-1}\phi_{\lambda}(\mathbf{r}_2)\phi_{\rho}(\mathbf{r}_2). \tag{5}$$

We use atomic units, in which $m_e = \hbar = e = 4\pi\epsilon_0 = 1$.

The total electronic energy in Hartree–Fock theory is given by:

$$E_{\mathrm{el}} = \frac{1}{2}\sum_{\mu\nu\sigma}\left[P^{\sigma}_{\mu\nu}(H_{\mu\nu} + F^{\sigma}_{\mu\nu})\right] \tag{6}$$

and it is clear that, in principle, a large number (N^4, where N is the number of basis orbitals) of two-electron integrals will have to be calculated before we obtain the Fock matrix or the electronic energy.

The zero-differential-overlap (ZDO) approximation (Parr 1952) consists of the neglect of a large number of these integrals and has two parts. The first part of the approximation assumes orthogonality between basis functions, i.e. replaces $S_{\mu\nu}$ by $\delta_{\mu\nu}$; the second part assumes

$$(\mu\nu|\lambda\rho) = (\mu\mu|\lambda\lambda)\delta_{\mu\nu}\delta_{\lambda\rho}. \tag{7}$$

These approximations should be invariant under rotation of local coordinate axes (producing mixing of the p orbitals) or hybridization (which will mix s and p orbitals of the same principal quantum number). This invariance is discussed more fully by Pople

and Beveridge (1970) and requires that the Coulomb integral $(\mu\mu|\lambda\lambda)$ be independent of the angular dependence of the basis functions; it is therefore a consequence of the ZDO approximation that we can express all Coulomb integrals in terms of s orbitals and they will be functions of interatomic distance only.

The next step is to choose the matrix elements that are retained in the ZDO approximation by selected fits to experimental data. A number of fitting schemes have been proposed; those used here are CNDO/2 (the original CNDO method is no longer used, and the qualification '/2' will henceforth be dropped) and INDO. CNDO (complete neglect of differential overlap) assumes the ZDO approximation completely, while INDO (intermediate neglect of differential overlap) retains all one-centre, two-electron integrals and assumes ZDO only for two-centre integrals. The only extra integrals that INDO retains are one-centre exchange integrals of the form $(\mu\lambda|\mu\lambda)$.

Further approximations of the two methods are involved in calculating the Hamiltonian matrix elements, and are outlined by Pople and Beveridge (1970). CNDO and INDO calculate two-centre terms in the same manner, and so the two-centre components of the Fock matrices will differ only in that the bond order matrices will not be the same. The open-shell Fock matrix elements in INDO are:

$$F^{\sigma}_{\mu\mu} = U_{\mu\mu} + \sigma_{\lambda \text{ on A}}\left[P_{\lambda\lambda}(\mu\mu|\lambda\lambda) - P^{\sigma}_{\lambda\lambda}(\mu\lambda|\mu\lambda)\right] + \sum_{\text{B}\neq\text{A}}(P_{\text{BB}} - Z_{\text{B}})\gamma_{\text{AB}} \tag{8a}$$

$$F^{\sigma}_{\mu\nu} = (2P_{\mu\nu} - P^{\sigma}_{\mu\nu})(\mu\nu|\mu\nu) - P^{\sigma}_{\mu\nu}(\mu\mu|\nu\nu) \qquad \mu,\nu \text{ on same atom} \tag{8b}$$

$$F_{\mu\nu} = \tfrac{1}{2}K_{\text{AB}}S_{\mu\nu}(\beta^{0}_{\text{A}} + \beta^{0}_{\text{B}}) - P^{\sigma}_{\mu\nu}\gamma_{\text{AB}} \qquad \mu \text{ on A},\ \nu \text{ on B} \tag{8c}$$

where $P_{\text{AA}} = \sum_{\mu \text{ on A}} P_{\mu\mu}$ and Z_{B} is the charge on the core of atom B.

The terms in these matrix elements fall into three categories:

(i) $\{U_{\mu\mu}\}$, $\{\beta^{0}_{\text{A}}\}$ and the one-centre, two-electron integrals are constant parameters of the method and can be set at the start of the calculation. The integrals can be calculated *ab initio* while standard values, optimized for a broad range of compounds, exist for the other parameters (Pople and Beveridge 1970); note that *no* parameters are chosen explicitly to optimize the results of the calculations on conjugated polymers reported in the following paper. K_{AB} is chosen (entirely empirically) to be unity, unless either atom A or atom B is from the third row of the periodic table, in which case $K_{\text{AB}} = 0.75$.

(ii) $\{P_{\mu\nu}\}$ etc need to be recalculated whenever we update our estimate of the wavefunction.

(iii) $\{S_{\mu\nu}\}$ and $\{\gamma_{\text{AB}}\}$ also need to be recalculated, but in this case they depend on the estimated atomic geometry rather than directly on the wavefunctions.

3. The total energy and atomic forces

The total energy in INDO is given by the expression:

$$E = \sum_{\mu} P_{\mu\mu}\left(U_{\mu\mu} - \sum_{\text{B}\neq\text{A}} Z_{\text{B}}\gamma_{\text{AB}}\right) + \frac{1}{2}\sum_{\mu}\sum_{\lambda \text{ on A}}\left[P_{\mu\mu}P_{\lambda\lambda} - \sum_{\sigma}(P^{\sigma}_{\mu\lambda})^{2}\right](\mu\mu|\lambda\lambda)$$
$$+ \frac{1}{2}\sum_{\mu}\sum_{\lambda \text{ on B}}\left[P_{\mu\mu}P_{\lambda\lambda} - \sum_{\sigma}(P^{\sigma}_{\mu\lambda})^{2}\right]\gamma_{\text{AB}}$$

$$+\frac{1}{2}\sum_{\mu}\sum_{\nu\,\mathrm{on\,A}}\left[2(P_{\mu\nu})^2-\sum_{\sigma}((P^{\sigma}_{\mu\nu})^2+P^{\sigma}_{\mu\mu}P^{\sigma}_{\nu\nu})\right]\gamma_{\mathrm{AB}}$$
$$+\frac{1}{2}\sum_{\mu}\sum_{\nu\,\mathrm{on\,B}}K_{\mathrm{AB}}S_{\mu\nu}(\beta^0_{\mathrm{A}}+\beta^0_{\mathrm{B}})P_{\mu\nu}+\sum_{\mathrm{A}}\sum_{\mathrm{B<A}}Z_{\mathrm{A}}Z_{\mathrm{B}}R^{-1}_{\mathrm{AB}} \tag{9}$$

Orbital μ is attached to atom A and it is understood that a summation over two orbitals or atoms explicitly *excludes* the case for which they are the same. The derivative of the total energy with respect to a general atomic coordinate X_i is somewhat simpler, since of the electronic parameters only $\{S_{\mu\nu}\}$ and $\{\gamma_{\mathrm{AB}}\}$ actually involve two-centre integrals:

$$\frac{\partial E}{\partial X_i}=-\sum_{\mu}\sum_{\mathrm{B}\neq\mathrm{A}}P_{\mu\mu}Z_{\mathrm{B}}\frac{\partial\gamma_{\mathrm{AB}}}{\partial X_i}+\frac{1}{2}\sum_{\mu}\sum_{\lambda\,\mathrm{on\,B}}\left[P_{\mu\mu}P_{\lambda\lambda}-\sum_{\sigma}(P^{\sigma}_{\mu\lambda})^2\right]\frac{\partial\gamma_{\mathrm{AB}}}{\partial X_i}$$
$$+\frac{1}{2}\sum_{\mu}\sum_{\nu\,\mathrm{on\,B}}K_{\mathrm{AB}}\frac{\partial S_{\mu\nu}}{\partial X_i}(\beta^0_{\mathrm{A}}+\beta^0_{\mathrm{B}})P_{\mu\nu}-\sum_{\mathrm{A}}\sum_{\mathrm{B<A}}Z_{\mathrm{A}}Z_{\mathrm{B}}R^{-2}_{\mathrm{AB}}\frac{\partial R_{\mathrm{AB}}}{\partial X_i}$$
$$=-\frac{1}{2}\sum_{\mu}\sum_{\lambda\,\mathrm{on\,B}}\sum_{\sigma}[(P^{\sigma}_{\mu\lambda})^2]\frac{\partial\gamma_{\mathrm{AB}}}{\partial X_i}+\frac{1}{2}\sum_{\mu}\sum_{\nu\,\mathrm{on\,B}}K_{\mathrm{AB}}\frac{\partial S_{\mu\nu}}{\partial X_i}(\beta^0_{\mathrm{A}}+\beta^0_{\mathrm{B}})P_{\mu\nu}$$
$$-\sum_{\mathrm{A}}\sum_{\mathrm{B<A}}\left(Z_{\mathrm{A}}Z_{\mathrm{B}}R^{-2}_{\mathrm{AB}}\frac{\partial R_{\mathrm{AB}}}{\partial X_i}-P_{\mathrm{AA}}P_{\mathrm{BB}}\frac{\partial\gamma_{\mathrm{AB}}}{\partial X_i}\right)$$
$$-\sum_{\mathrm{A}}\sum\mathrm{B}\neq\mathrm{A}P_{\mathrm{AA}}Z_{\mathrm{B}}\frac{\partial\gamma_{\mathrm{AB}}}{\partial X_i}. \tag{10}$$

Equation (10) makes the physical meaning of each term clear: the first term represents the force due to the exchange interaction between electrons on atoms A and B, the second represents the electronic overlap, the third the electron–electron and core–core repulsion and the fourth the attraction between electrons on atom A and the core of atom B. Exactly the same expression applies for CNDO.

We have assumed that we can neglect the derivatives of the bond order matrices in calculating the energy derivatives. If we were using the full, many-electron Hamiltonian and the exact eigenfunctions, this neglect would be justified by the Hellman–Feynman theorem. It has been shown by Slater (1974) that this assumption is also valid in Hartree–Fock theory, provided that the eigenfunctions are exact (Slater's proof is outlined in the case of $X-\alpha$ theory but since it relies only on the wavefunctions being calculated by a variational principle for its validity, it applies in Hartree–Fock theory also). We are tacitly assuming, therefore, that the instantaneous eigenfunctions remain very close to the Hartree–Fock ground state during the calculation. The failure of this approximation would be reflected by a failure of energy conservation in undamped molecular dynamics. We return to this point below.

The force acting on an atom is given by $F=-\nabla E$ so, using M_i for the mass of atom i and X_i as an atomic coordinate:

$$M_i\ddot{X}_i=-\frac{\partial E}{\partial X_i}. \tag{11}$$

Using the Verlet algorithm (Verlet 1967) to expand the atomic coordinates as a second-order Taylor series, using a time step Δt and damping by a factor ξ (i.e. reducing all

atomic velocities by a factor ξ at each step), we obtain:

$$X_i(t+\Delta t) = X_i(t) + \xi V_i(t)\Delta t - \frac{1}{M_i}\frac{\partial E}{\partial X_i}\bigg|_t (\Delta t)^2$$
$$V_i(t) = \frac{1}{\Delta t}[X_i(t) - X_i(t-\Delta t)]. \tag{12a}$$

Efficient choice of Δt and ξ is important if we are to reach a minimum-energy geometry as quickly as possible; a guide to how this may be done is given in appendix A. We have found that a more effective choice of numerical integration algorithm for the ionic equations of motion, particularly when no damping is applied, is that due to Beeman (1976), which uses information from the last three evaluations of the forces in the calculation of the new ionic positions:

$$X_i(t+\Delta t) = X_i(t) + \xi V_i(t)\Delta t - \frac{1}{6M_i}\left(4\frac{\partial E}{\partial X_i}\bigg|_t - \frac{\partial E}{\partial X_i}\bigg|_{t-\Delta t}\right)(\Delta t)^2$$
$$V_i(t) = V_i(t-\Delta t) - \frac{1}{6M_i}\left(2\frac{\partial E}{\partial X_i}\bigg|_t + 5\frac{\partial E}{\partial X_i}\bigg|_{t-\Delta t} - \frac{\partial E}{\partial X_i}\bigg|_{t-2\Delta t}\right)\Delta t. \tag{12b}$$

This form produces ionic trajectories almost indistinguishable from those given by the Verlet algorithm (12*a*) but gives superior energy conservation. This issue is discussed further in Appendix B.

We are now (in principle) able to perform the simulated annealing process which minimizes the energy of the system. All that remains is to calculate the overlap and Coulomb integrals $S_{\mu\nu}$, γ_{AB} and their derivatives with respect to atomic coordinates. The methods used are outlined below, after a brief description of the STO we use as a basis set.

4. The basis functions: Slater-type orbitals and their derivatives

Slater-type orbitals $\phi_{nlm\zeta}$ are defined in terms of three quantum numbers and an orbital exponent:

$$\phi_{nlm\zeta} = N(n)Y_{lm}r^{n-l}\exp(-\zeta r). \tag{13}$$

The orbital exponent, ζ, is found empirically; in particular, in CNDO and INDO it is treated as a function of n only. The radial normalization factor $N(n)$ is:

$$N(n) = [(2\zeta)^{2n+1}/(2n)!]^{1/2}. \tag{14}$$

We use real STO with angular parts chosen such that the orbitals point along clearly defined directions. These real combinations are given by Wallace (1989).

We obtain the derivatives of the Coulomb integrals γ_{AB} with respect to the atomic positions analytically (Wallace 1989), while the derivatives of the overlap matrix elements $S_{\mu\nu}$ may be obtained by differentiating the wavefunctions, expressing the result in terms of new Slater-type orbitals and integrating over these in the usual way. Thus

$$\frac{\partial S_{\mu\nu}}{\partial X_2} = -\int \phi_\mu(\boldsymbol{r}-\boldsymbol{R}_1)\frac{\partial \phi_\nu(\boldsymbol{r}-\boldsymbol{R}_2)}{\partial x}\,\mathrm{d}^3r$$
$$= -\sum_\alpha d_{\nu\alpha}S_{\nu\alpha} \tag{15}$$

where

$$\frac{\partial \phi_\nu}{\partial x} = -\sum_\alpha d_{\nu\alpha}\phi_\alpha. \tag{16}$$

The coefficients $d_{\nu\alpha}$ are given by Wallace (1989). This method was first suggested by Pulay and Torok (1973).

5. Calculation of the wavefunction

In the original method of Car and Parrinello (1985) the wavefunctions are calculated by a simulated molecular dynamical (MD) method. Just as the atomic coordinates are determined by equation (12*a*) or (12*b*), the principle can be extended to calculation of the wavefunctions by replacing the coordinate X_i by $c_{\mu i}$ and introducing a fictitious mass m for the wavefunction. The evolution is, however, constrained by the requirement that the wavefunctions remain orthonormal; if the number of basis functions is N and the number of occupied orbitals M, this imposes $M(M+1)/2$ conditions of the form:

$$\sum_\mu c_{\mu i}c_{\mu j} = \delta_{ij}. \tag{17}$$

Each condition requires $O(N)$ multiplications and additions, so the total number of operations required is $O(M^2N)$. Straightforward matrix diagonalization requires $O(N^3)$ operations (although some modern routines can take $O(N^2 \log N)$), so there is a substantial advantage in the Car–Parrinello method if $N \gg M$. If, however, we use an STO basis, the numbers of basis functions and of occupied orbitals are similar and part of the advantage in the MD technique is lost.

A similar problem involving the application of external constraints to a system has been examined by Ryckaert *et al* (1977) who considered the dynamics of small hydrocarbon molecules under the constraint of fixed bond lengths. The constraints must be maintained *exactly* throughout the calculation, even though the wavefunctions will only satisfy the equations of motion to limited accuracy (i.e. to $O(\Delta t)^2$ if the Verlet algorithm is used). They proposed two methods for ensuring orthogonality: the constraints can be satisfied simultaneously by a matrix method, or in turn, by allowing the wavefunctions to move freely, and then orthogonalizing. In view of the difficulties involved in these schemes, and also of the reduced benefit of the molecular-dynamical approach to solving for the wave function when the total number of basis states does not greatly exceed the number of orbitals, we have adopted the conceptually simpler solution of diagonalizing the Fock matrix a fixed number of times at each geometry, using the resulting eigenvectors to construct a new bond-order matrix and re-calculate the forces on each ion for the next iteration. We expect this to work if, roughly speaking, the time step used for the atomic motion is sufficiently small that the change in atomic positions does not pull the Fock matrix away from self-consistency faster than diagonalization at constant geometry would push it towards self-consistency.

6. Extensions to the relaxation routines

It is a simple process to extend the relaxation method to include consideration of various extra forces and constraints. Those implemented at present, with brief details of how they affect the calculation of the molecular energy and the atomic forces, are summarized below.

6.1. External forces

It may sometimes be desirable to apply external forces to some of the atoms in a molecule (in order to examine the behaviour of a molecule under pressure, for example, or to prevent an unstable system from breaking apart). This is trivially done by adding the force directly to that calculated using equation (10) and by adding a term $-\sum_i F_i R_i$ to the total energy.

6.2. Applied force fields and constraints

When considering the behaviour of certain molecules (in particular biological molecules, but the same principle could apply to the study of adsorbed gas molecules) it may be advantageous to study them in conjunction with some substrate (typically, in the case of biological molecules, a receptor of some kind). It may not be feasible directly to incorporate the substrate molecule into the relaxation calculation (either because its nature is not known, or because it is too large for such a calculation to be worthwhile), so the facility has been added to specify an effective force field to represent the substrate. It is also possible to constrain the relaxation by preventing individual atoms from moving in particular directions.

6.3. Electric fields

The behaviour of molecules in the presence of an electric field is also easily examined. The field need not be uniform throughout the molecule, but there is the constraint that the field at an atom must not vary significantly over a distance shorter than the relevant orbital exponent. If we are concerned with the field due to a point charge, for example, this condition will be satisfied provided that the distance from any atom to the charge is much greater than the orbital exponent (typical orbital exponents are in the range 1–2 au, or about 0.5–1.0 Å, so this should not normally pose a problem). Should it be necessary to work with fields that do vary significantly over a shorter distance than this, the calculations below will need to be repeated without making the approximation that the potential can be expanded to first order about an atomic nucleus.

Application of an electric field is the only one of these extensions that will directly affect the wave functions. The Hamiltonian must be modified to take account of the added potential by changing its elements by:

$$\delta H_{\mu\nu} = -\langle\mu|V|\nu\rangle. \tag{18}$$

We write $V(\boldsymbol{R}+\boldsymbol{r}) = V(\boldsymbol{R}) - \epsilon(\boldsymbol{r})\boldsymbol{r}$, where $\boldsymbol{R}$ represents the nuclear position, $\boldsymbol{r}$ the electronic coordinates relative to $\boldsymbol{R}$ and ϵ is the electric field at the nucleus in atomic units. The only non-zero matrix elements are diagonal elements of the form $\langle\mu|V(R)|\nu\rangle$ and off-diagonal elements of the form $\langle s|x|p_x\rangle$, where the orbitals are centred on the same atom (the two-centre terms are negelected in the ZDO approximation). The first of these integrals is trivial, as $V(R)$ is independent of r, while the second is easily calculated:

$$\langle s|x|p_x\rangle = (2n+1)\epsilon_x/(2\zeta\sqrt{3}). \tag{19}$$

The electric field also contributes $Z\epsilon(R)$ to the force on an atomic core and $ZV(R)$ to the core energy. The adjustments to the Hamiltonian will affect the energy of the molecule but we must also alter the forces explicitly, since our previous assumption that the Hamiltonian matrix elements were independent of position is no longer valid. It is necessary to add a force $-P_{AA}\epsilon(R)$, with P_{AA} as defined following equation (8).

6.4. Fixing hydrogen atoms to their hosts

In a number of cases it is disadvantageous for the hydrogen atoms in a molecule to be allowed to move freely; for example, the geometry optimization would be accelerated by using a large time step, but this time step would lead to instability in the high-frequency oscillations within the molecule, which will normally be those oscillations involving hydrogen atoms. Accordingly, the facility to freeze hydrogen atoms to their host atoms has been included; if necessary, the positions of the hydrogen atoms can be optimized in a separate calculation. Note that the hydrogen atoms feel no forces in this case but move in parallel to the host atom.

7. Implementation

The relaxation program has been implemented on an 8 MHz IBM-PC for molecules of up to 26 atoms or 65 orbitals, and on an IBM 3084 mainframe for molecules of up to 100 atoms or 300 orbitals (the low ratio of orbitals required per atom is a consequence of the large proportion of hydrogen atoms in the molecules under consideration, since only a valence basis set is used). The latter version has also been implemented on the CRAY-2 at Harwell. The memory required is rather less than $100N^2$ bytes, where N is the number of basis orbitals, and the mainframe version takes up approximately 7.5 Mbytes of storage. It is however the CPU time required that is the principal factor limiting the size of system that can be treated. For large systems this will increase as N^3, as the matrix diagonalization is the time-limiting step, but when considering small systems the calculation of overlap integrals and their derivatives will continue to be an important element and the calculation time will increase less quickly. Since overlap integrals may in general be assumed to be small for interatomic separations of greater than about 5 Å (they contain a factor $\exp(-2\zeta R)$, where the orbital exponent ζ is greater than 1 a.u. for most of the atoms we consider), the facility is included to specify a limit of atomic separation beyond which all overlap integrals will be neglected and all Coulomb integrals replaced by $1/R$; this can lead to considerable savings of time when considering long molecules such as the polymer models investigated in the following paper. That the 5 Å limit suggested above is a reasonable approximation can be seen by examining figure 1, which plots two sample Coulomb integrals and has a curve of $1/R$ for comparison.

8. Applications of the method

Our method was originally developed to study the molecular structure and charge-chain coupling in conjugated polymers. These studies are described in the following paper. However, its speed and flexibility mean that it can be used to investigate the ground state properties of any systems which are well treated by CNDO and INDO; these include most organic molecules. Since the cost of optimizing the geometry of a molecule has been made comparable to the cost of calculating its wavefunctions at fixed geometry, it is now feasible to calculate the dipole moments of molecules in their optimal geometry state (section 8.2). This enables us to understand better the strengths and weaknesses of the CNDO method.

By applying a uniform electric field to the molecule under consideration we can find theoretical polarizabilities in a non-perturbative manner and account for that part

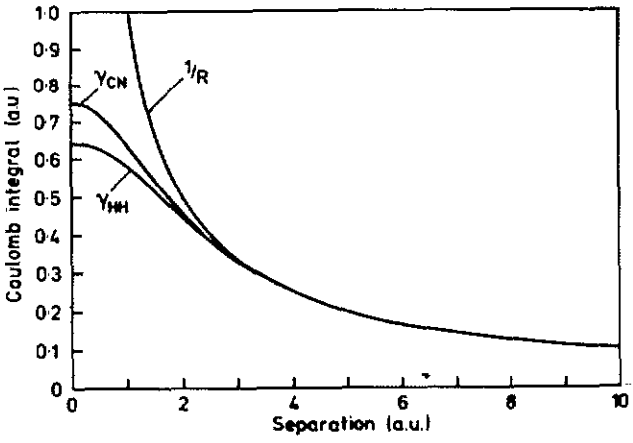

Figure 1. Coulomb integral $\gamma_{AB}(R)$ against atomic separation R for the cases (a) γ_{HH} (b) γ_{CN}. Curve (c) is the long-distance limit $\gamma = 1/R$.

of the polarizability due to a molecule's ability to distort in a field. The results of these calculations are given in section 8.3 and reproduce well the self-consistent perturbative results in the cases in which these are available, although a slight improvement on the perturbative results is noticeable.

The study of molecular vibrations is also possible in a number of cases and may be useful where a valence force potential model is not suitable (see paper II). Some simple examples are given in section 8.4 which demonstrate the consistent overestimation of phonon frequencies by CNDO.

8.1. Geometry optimization

CNDO has had much success in predicting ground state geometries for a range of (mostly organic) molecules (Pople and Beveridge 1970 section 4.2, Sadlej 1985 section 5.4). However, the methods used have often been time-consuming and unreliable. These have included discrete stepping through candidate geometries, (Pople and Beveridge 1970); minimization methods which involve calculating only the energy at each geometry (Powell 1964); and techniques involving calculating the total energy and its first derivative at each geometry (McIver and Komornicki 1971). The latter authors compared their method with that of Powell, using the geometry optimization of ethene as an example. The starting geometry had a C = C bond length of 1.34 Å, C–H bond lengths of 1.10 Å and all bond angles were 120°. The convergence criterion was that the change in any atomic coordinate must not exceed 0.01 Å in any step. The Powell method required 37 calculations of the total energy before the geometry met this criterion, while that of McIver and Komornicki required only 7 such calculations. Each energy calculation requires about 5 matrix diagonalizations (they did not specify the precision to which they required the energy), so the two methods required approximately 185 and 35 matrix diagonalizations, respectively, while that used here required 11 diagonalizations for the same degree of convergence.

Two examples of results generated by the geometry optimization process are given. The series obtained by the increasing fluorination of methane is examined (table 1) and the ground state geometry of methanol is obtained (table 2). In the former case the trends observed experimentally are reproduced well qualitatively, albeit less well quantitatively.

Table 1. Calculated and experimental geometries for the fluoromethanes. Experimental results are given in brackets; for the original references, see table 4.7 of Pople and Beveridge (1970). Experimental values for the C–H bond length and the H–C–H angle in CH_2F_2 are not available.

	Bond lengths (Å)		Bond angles (degrees)	
	C–H	C–F	H–C–H	F–C–F
CH_4	1.114 (1.093)		109.5 (109.5)	
CH_3F	1.118 (1.105)	1.344 (1.385)	109.7 (109.9)	
CH_2F_2	1.121	1.342 (1.36)	110.9	102.0 (108.5)
CHF_3	1.123 (1.098)	1.341 (1.332)		106.3 (108.8)
CF_4		1.338 (1.317)		109.5 (109.5)

Table 2. Calculated and experimental ground-state geometries of methanol. Experimental results are those of Ivash and Dennison (1953); asterisks denote assumed values. It is not clear how Ivash and Dennison reconcile their assumption that the methyl group is perfectly tetrahedral with their non-zero value for the angle θ.

	Theory (CNDO, this work)	Experiment
Bond lengths (Å)		
C–H	1.121	1.09*
C–O	1.368	1.43
O–H	1.033	0.94
Bond angles (degrees)		
C–O–H	105.2	105.9
H–C–H	108.3	109.5*
H–C–O	108.4, 111.7	109.5*
H_3–C–O angle θ	2.2	3.2

The ground-state geometry of methanol has been examined experimentally by Ivash and Dennison (1953) and agrees well with that predicted by CNDO (it is well known that CNDO tends to over-predict the O–H bond length by up to 0.1 Å). It is correctly predicted that the staggered form is more stable (figure 2), and that the methyl group is bent away from the C–O bond by a small angle, labelled α in the figure (see table 2). The value obtained by Ivash and Dennison is slightly larger than that predicted by CNDO, but relied for its derivation on the assumption that the methyl group was purely tetrahedral, with a C–H bond length 1.09 Å. To reach an optimal geometry to within the convergence criterion of McIver and Komornicki (see above) required only 12 matrix diagonalizations, the equivalent of just three energy calculations at fixed geometry.

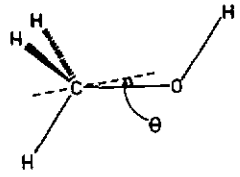

Figure 2. Geometry of methanol (see table 1). Note that the axis of the methyl group is shifted slightly away from the C–O bond.

8.2. Charge distribution and dipole-moment calculations

In this section we examine how the successful CNDO predictions of molecular dipole moments (table 4.18 Pople and Beveridge 1970) are altered when these are evaluated at the minimum-energy CNDO geometry, rather than with standard values for bond angles and bond lengths (Pople and Gordon 1967). This enables us to see to what extent the discrepancies in earlier work are due to the CNDO method, as opposed to the choice of geometry.

It should be noted that the dipole moment associated with a bond actually varies rather slowly with the bond length. Consideration of an HF molecule with different bond lengths shows that the charge stored on each atom is slightly reduced as the bond length increases and that the dipole moment associated with the orbitals forming the bond is reduced more substantially, leaving the overall dipole moment changed by at least an order of magnitude less (proportionately) than the bond length (table 3).

Table 3. Dipole moment of HF as a function of bond length.

Bond length (Å)	Atomic charge	Dipole moment (D)		
		Atoms	Bond	Total
0.90	0.233	1.008	0.839	1.847
0.95	0.229	1.047	0.808	1.855
1.00	0.226	1.087	0.774	1.861
1.05	0.223	1.126	0.740	1.867
1.10	0.221	1.167	0.705	1.872

The bond angles in a molecule may affect the predicted dipole moment, however, and the standard geometrical models fail to account for any change in these from their perfect (tetrahedral, trigonal or linear) values. One obvious case to consider is the series $H_2O \rightarrow CH_3OH \rightarrow CH_3OCH_3$, where steric effects open out the bond angle at the oxygen with increasing size of the attached groups. CNDO correctly predicts that the dipole moment should decrease along this series but underestimates the extent of this decrease and somewhat overestimates the dipole moments themselves (table 4). Using optimized geometries rather than the standard geometries does improve the results somewhat, but this correction is not sufficient to account for the discrepancy and it is necessary to conclude that the error is inherent in the method.

Table 4. Theoretical and experimental dipole moments (debyes). The original references for the experimental data are given in table 4.18 of Pople and Beveridge (1970).

	Standard geometry	Optimized geometry	Experiment
H_2O	2.10	2.10	1.85
CH_3OH	1.94	1.85	1.69
CH_3OCH_3	1.83	1.75	1.30

Finally we consider the fluoromethanes, whose geometries we discussed above. The dipole moments of fluoromethane (CH_3F) and fluoroform (CHF_3) are predicted, using the standard geometries, to be very similar, as should be the case if each fluorine atom

attracts an equal charge away from the central carbon atom, irrespective of how many other fluorine atoms are already attached to it. Experimentally, the dipole moment of CH_3F is rather higher (1.855 D compared with 1.645 D), presumably because the fluorine atoms find it more difficult to attract charge when there are more of them. Use of the optimized geometries, however, predicts the reverse (dipole moments of 1.60 D and 1.98 D for CH_3F and CHF_3 respectively) and it is clear that this is due to the underprediction of the F–C–F bond angle in CHF_3 (table 1).

8.3. Molecular polarizabilities

Calculations of molecular polarizabilities have previously been carried out within the CNDO approximation by a perturbative method, assuming fixed molecular geometry (Davies 1969). As with the study of dipole moments (section 8.2) it is interesting to see how the use of optimized molecular geometries affects the results obtained. The method used here is non-perturbative, in that it involves merely optimizing the geometry of a molecule with an externally applied electric field and measuring the change in dipole moment associated with the field. A polar molecule must be held fixed in some way if the polarizability at an angle to the dipole moment is to be measured, as the molecule will otherwise rotate to bring its dipole moment towards the direction of the applied field. However, when measuring the polarizability along the axis of the moment, or that of a non-polar molecule, this constraint is not necessary and the molecule can be allowed to relax completely.

Table 5. Polarizability of HF as a function of bond length.

Bond length (Å)	α_1	α_2	Total α (Å^3)
0.90	0.32	-0.02	0.30
0.95	0.38	-0.02	0.36
1.00	0.44	-0.02	0.43
1.00*	0.57	-0.05	0.51
1.05	0.51	-0.02	0.50
1.10	0.59	-0.01	0.58

* denotes that the molecule was allowed to relax. The equilibrium bond length in HF is calculated to be 0.99985 Å and this increases by approximately 3 Å per atomic unit of field for small fields.

The polarizability of a molecule is a much more sensitive function of the geometry than the dipole moment, as can be seen if we consider the case of hydrogen fluoride again (table 5). The components α_1 and α_2 of the polarizability correspond to changes in the two components of the dipole moment, those parts due, respectively, to charge separation between the atoms and to polarization of the bond itself (as in table 3). (A change in dipole moment of 1 D per atomic unit of field corresponds to a polarizability volume of 0.0584 Å^3.)

It is clear (table 5) that the part of a molecule's polarizability due to the polarizability of the interatomic bonds themselves is insignificant within the CNDO approximation, and that the important term arises from the movement of charge between the two atoms. Allowing the molecule to distort may make a significant contribution to the molecular polarizability when the molecule is already highly polar (as in this case) or when the effective force constant preventing distortion is small, which might be the case in some biological molecules.

Table 6. Theoretical and experimental molecular polarizabilities (Å^3).

		CNDO[a]	CNDO[b]	CNDO[c]	*Ab initio*[d]	Experiment[e]
H_2	α_{xx}	0.21	1.60	0.46	1.29	0.93
	α_{yy}	0.00	1.20	0.00	0.80	0.72
N_2	α_{xx}	1.10		1.64	4.67	2.38
	α_{yy}	0.40		0.82	1.27	1.45
HF	α_{xx}	0.32	0.63	0.51	0.79, 0.86[f]	0.96
	α_{yy}	0.03	0.22	0.03	0.36, 0.62	0.72
C_2H_4	α_{xx}	2.40	4.08	2.55		5.61
	α_{yy}	1.10	2.86	1.15		3.59* 3.96[g]
	α_{zz}	0.50	1.77	0.46		3.59* 3.38[g]
C_2H_6	α_{xx}	1.26	3.78	1.49		5.48
	α_{yy}	1.23	3.76	1.40		3.97

[a] Davies (1969).
[b] Davies (1969) with the inclusion of 2p orbitals on the hydrogen atoms.
[c] Self-consistent calculations (this work).
[d] Kolker and Karplus (1963) except where stated.
[e] Landolt and Bornstein (1951) except where stated.
[f] Stevens and Lipscomb (1964).
[g] Derived using the empirical bond polarizabilities given by Denbigh (1940).
* Assuming rotational symmetry.

CNDO quantitative predictions of molecular polarizabilities are poor, presumably owing to its failure to treat bond polarizabilities in a satisfactory manner. This is principally a consequence of the use of a valence-only basis set; studies by Davies (1969) of the effect of including 2p orbitals on hydrogen atoms lead to slightly improved results but the correlation with experimental values is still, at best, tenuous. The principal values of the polarizability tensors of various molecules are given in table 6. It is clear that a significant improvement may be obtained by using an *ab initio* method and a larger basis set; both sets of authors using this method obtained results in much better agreement with experiment than the CNDO results, except in the case of the polarizability of N_2 along its axis (the axes are defined such that the molecular axis is the x axis, and that the ethene molecule lies in the x–y plane). The basis sets they use are substantially larger than the STO valence basis set used here. In particular, the CNDO results are very poor when describing the off-axis polarizabilities; as mentioned before, CNDO only accounts adequately for polarizabilities due to physical charge separation and this is not the major contribution to the polarizability perpendicular to a bond.

However, the possibility of using CNDO to predict molecular polarizabilities should not be entirely excluded; although the values it predicts are too low, the underprediction is fairly consistent and certainly sufficiently regular to allow a reasonable prediction of the experimental value. If we look at the mean polarizabilities of a range of organic molecules (table 7) we can see that the underprediction leads to theoretical values that are between 24% and 33% of the experimental results in all but one case.

8.4. Vibrational frequencies

CNDO will rarely be the optimal method for the calculation of vibrational frequencies. Methods using valence force potentials exist (for a review of the use of valence force potentials, see Allinger 1976), and the force constants used therein have been well

Table 7. Mean polarizabilities (Å^3).

	CNDO	Experiment[a]	Ratio CNDO: Experiment
NH_3	0.64	2.26	0.29
HCN	0.84	2.59	0.32
CH_4	0.63	2.60	0.24
CCl_4	3.02	10.50	0.29
C_2H_2	0.91	3.33	0.27
C_6H_6	4.14	10.32	0.40
C_2H_4	1.39	4.26	0.33
C_2H_6	1.43	4.72	0.30

[a] Landolt and Bornstein (1951).

parametrized to fit existing data, resulting in the ability to generate an accurate set of theoretical frequencies for most molecules.

In certain special cases, however, it will not be possible to use valence force potentials. One such case is the treatment of vibrations in a charged or electronically excited state (since the bond orders, and hence the force constants, will change on excitation or charging) and another is the study of conjugated polymers. Although some computer programs using valence force potentials can handle systems with conjugated π electrons, they mostly do so by calculating a bond order for each bond (within Hückel theory) and using an empirical bond order–force constant relationship to derive a force constant. This fails to take into account properly electron–phonon coupling and is thus expected to overestimate the frequencies of the Raman-active phonons in polyacetylene (see paper II).

The calculation of vibrational frequencies within CNDO is a problem that has been studied by Pulay (1969, and a number of subsequent papers), who calculated force constants by a double differentiation process. Performing both differentiations analytically is not feasible and performing them both numerically is immensely time-consuming (although Mori and Kurihara (1988) have recently studied the localized modes around a soliton in t-PA within the MNDO approximation by performing both differentiations numerically), so Pulay suggested performing the first differentiation analytically and the second numerically. Calculation of a complete force constant matrix by this method requires 3N total energy calculations, and for small molecules this presents no problem.

For large molecules, and particularly in cases for which we only require the frequencies of certain specific modes, it will be quicker to use the molecular dynamical method of this paper to allow the molecule to vibrate in real time and find the frequencies of the normal modes by Fourier transforming this vibration. The details of this method are outlined here, and it is applied to a few small molecules in order to compare the frequencies obtained with experiment. It should be stressed that, for molecules of the size considered in this section, the method of Pulay is more appropriate; only for large molecules does the real-time method lead to significant savings in computation.

The modes whose frequencies we require can be selected by careful choice of the initial geometry. To take a simple example, to find the frequency of the symmetric C–H stretch (the *breathing mode*) in methane requires a symmetric initial geometry, with the C–H bonds all slightly stretched. The total length of time over which the molecule must be allowed to vibrate depends on the precision to which we want the

frequency, and the choice of time step involves a trade-off between the extent to which too large a time step will degrade the harmonic motion of the system and the extra number of steps required if the time step is too small. A time step of 1 unit (where the program's natural unit of time is $\sqrt{m_p}$ atomic units, or 1.036 fs) is in general found to be suitable.

The example of the breathing mode in methane was used to illustrate the method. The molecule was allowed to vibrate for 200 time steps, and this means that values of the Fourier transform can be calculated at frequency intervals of 0.031 units (boundary conditions dictate that the frequency used for the transform must take the form $2n\pi/(N+1)\tau$). One unit of frequency corresponds to 5118 cm^{-1}, so the separation between successive frequencies is approximately 160 cm^{-1}. By simply noting the position of the peak, the frequency of the mode can be obtained to ± 80 cm^{-1}, which may be good enough for our purposes but can be improved significantly by looking more closely at the Fourier transform (figure 3) in the following manner.

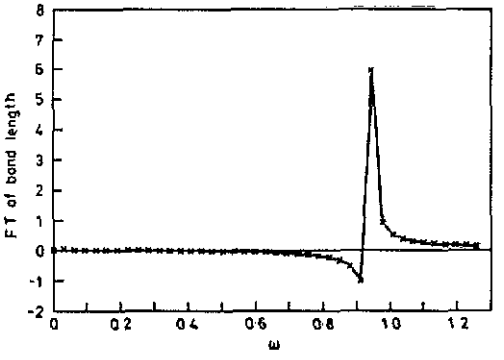

Figure 3. Fourier transform of the C–H bond length in methane obtained from a dynamical run. The line is a guide to the eye. Units are the natural units of the program in which $\omega = 1$ represents 5118 cm^{-1}, so the peak is observed at 4800 cm^{-1}.

Define an effective Fourier transform $F(\omega)$ by:

$$F(\omega) = \sum_n f(t_n)\cos(\omega t_n). \tag{20}$$

Then, if we replace the summation by an integral and assume that the displacement $f(t)$ takes the form $A\cos(\Omega t)$, we get (for $\omega \approx \Omega$):

$$F(\omega) \propto 1/(\omega - \Omega). \tag{21}$$

This changes sign as the estimated frequency, ω, passes Ω, and the ratio of the peak heights at either side of this sign change can give us the actual frequency, Ω, to much better precision than before. If we use ω_m to represent $2m\pi/(N+1)\tau$, and choose m such that Ω lies between ω_m and ω_{m+1}, we then have:

$$\frac{F(\omega_m)}{F(\omega_{m+1})} = \frac{\omega_m + 2\pi/(N+1)\tau - \Omega}{\omega_m - \Omega}. \tag{22}$$

The measured peak heights of figure 3 are -0.98 and 5.95, respectively, at $\omega = 0.911$ and 0.942, so the frequency of the vibration is calculated to be 0.938 units, equivalent

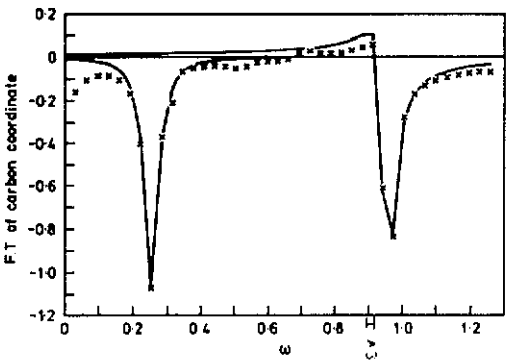

Figure 4. Fourier transform of one coordinate of the carbon atom in formaldehyde. The initial conditions were such that only the two antisymmetric normal modes are present. The peaks are not so sharp as in figure 3 but frequencies may be accurately extracted by fitting curves of the form given in (24); the solid lines are such fits for each of the two peaks. The units of frequency are as in figure 3 and the peaks occur at 1290 cm^{-1} (antisymmetric bend) and 4875 cm^{-1} (antisymmetric C–H stretch).

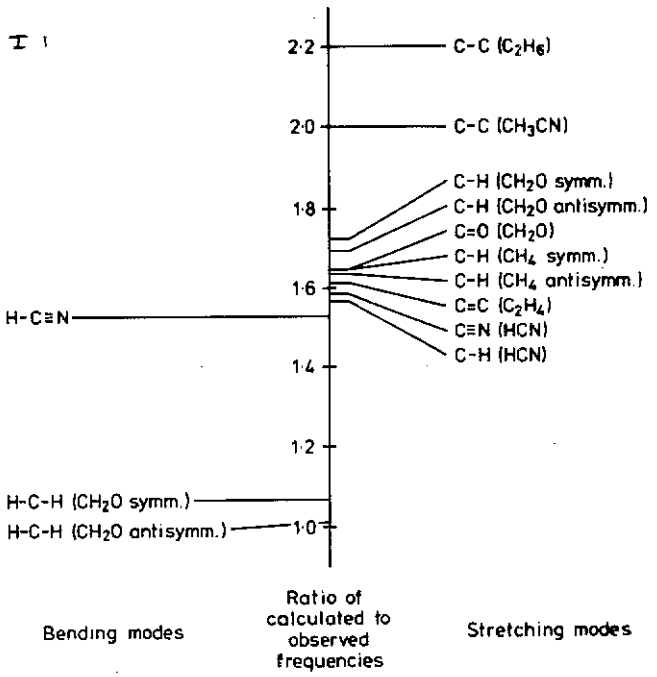

Figure 5. Diagrammatic representation of the amount by which vibration frequencies are over-predicted by CNDO. Note that the ratios are strongly clustered in a very narrow region except for the C–H bending modes (whose frequencies are only slightly over-predicted) and the C–C stretching modes (for which the over-prediction is rather greater than the norm). These ratios can be used to scale down the frequencies calculated by CNDO for other vibrations of similar type.

to 4800 cm^{-1}. Without this correction, we would have estimated 4825 cm^{-1}. This value is correct to better than ± 10 cm^{-1}. Sometimes the atomic motion is slightly damped, however, and the resulting Fourier transform is not as sharp as that of figure 3. It is still desirable to know the normal mode frequency to the same precision, however, and how this may be done is illustrated for the case of formaldehyde (CH_2O). An initial state with the antisymmetric modes excited was used, and the resulting Fourier transform is shown in figure 4. Assuming that the atomic displacement now

takes the damped form:

$$f(t) = A\cos(\Omega t)\exp(-kt) \tag{23}$$

with k small, it is easy to repeat the calculation of $F(\omega)$ and the result is (again for $\omega \approx \Omega$):

$$F(\omega) = S\frac{(\omega - \Omega) + Ck}{(\omega - \Omega)^2 + k^2} \tag{24}$$

where S is a constant and $C = \tan(\Omega\tau(N+1)/2)$. It is straightforward to fit the observed $F(\omega)$ values to a curve of this form and even a fit by eye can lead to a value of Ω precise to better than 10 cm^{-1}. In figure 4, the lines are fits by eye and the calculated vibrational frequencies are 1290 cm^{-1} and 4875 cm^{-1}, respectively.

Comparison between vibrational frequencies calculated using this method and their experimental values confirms that the theoretical values are, without exception, too large. This is expected, since CNDO overpredicts force constants by a factor typically between 2 and 3 (see e.g. table 5.4 Sadlej 1985, table 4.1b Pople and Beveridge 1970). Just as in the study of polarizabilities, however, systemic overprediction means that we can allow for it and adjust our calculated values accordingly. We examine the factor by which the frequencies are overpredicted in a few sample cases in table 8. In the main, the values of table 8 fall in the range 1.54 to 1.73, with the C–H bending mode values substantially lower and the C–C stretching mode values rather higher. They are shown in diagrammatic form as figure 5.

Table 8. Vibrational frequencies.

	Observed (cm^{-1})[a]	Calculated (cm^{-1}) (This work)	Ratio calculated: observed
HCN bend	712	1100	1.54
C≡N stretch	2089	3320	1.59
C–H stretch	3312	5190	1.57
CH_2O symmetric bend	1503	1610	1.07
antisymmetric bend	1280	1290	1.01
symmetric C–H stretch	2780	4810	1.73
antisymmetric C–H stretch	2874	4875	1.70
C=O stretch	1744	2880	1.65
CH_4 breathing mode	2914	4800	1.65
antisymmetric C–H stretch	3020	4950	1.64
C_2H_4 C=C stretch	1623	2640	1.62
C_2H_6 C–C stretch	993	2190	2.20
CH_3CN C–C stretch	918	1840	2.00

[a] Herzberg (1945).

9. Conclusion

We have described the principles and implementation of a method of determining equilibrium geometries and dynamics of molecules when their electronic structure is calculated using the CNDO and INDO semi-empirical methods. The resulting program

is sufficiently fast that it can be run on a PC for small molecules, and with a large computer it is able to tackle very complicated problems. Such an application, to the structure and dynamics of defects in conducting polymers, is described in the following paper (paper II).

The self-consistent geometry optimization process described here can be applied to the study of any system where electron–lattice coupling is important, subject to the condition that it be well described by a semi-empirical method similar to CNDO. This enables both the study of a wide range of classical defect theory and the examination of the behaviour of molecular systems in ground, excited or charged states.

Two further features of this method lend it to a number of additional areas of study: firstly, its dynamical nature means that chemical reaction pathways can be investigated; molecules can even be pushed towards each other in order to allow a kinetic barrier to be overcome or to simulate an applied pressure. Secondly, the flexibility of the method means that externally applied effects can be considered; the treatment of a receptor molecule when considering the behaviour of the neurotransmitter serotonin (Stoneham 1989) is just one form of external constraint that can be examined. Another area of study which has been suggested involves the use of the facility to apply a non-uniform electric field to the system under investigation in order to consider how the geometry of, for example, a biological molecule might be affected by the tip of a scanning tunnelling microscope, and thus to what extent such a method of measuring a molecule's structure would be useful (Ramos *et al* 1990).

Acknowledgments

DSW and AJF acknowledge the receipt of Research Studentships from the SERC and AJF thanks St John's College, Oxford, for the award of a Junior Research Fellowship. Part of this work was supported by the Underlying Research Programme of the UK Atomic Energy Authority and part by the Commission of the European Communities (contract No C11.0324).

Appendix 1. Damping of the atomic motion

Finding the minimum energy geometry of a system by a molecular dynamical method is strongly dependent for its efficiency on suitable choices of the time step and damping factor. It is intuitively obvious that if a single mode of vibration is present with frequency ω, the time step should be of order $1/\omega$; in this appendix we present a brief mathematical discussion of this point.

The iterative process for atomic relaxation leads to equation (12*a*) or (12*b*) of the main paper. We shall concentrate on (12*a*) in this appendix, although the argument in the case of (12*b*) is similar. If we assume, for simplicity, that we are dealing with one normal mode only, with equilibrium displacement zero, and that the time step used is sufficiently small that the Fock matrix remains close to its self-consistent value throughout the minimization process (which is essentially the Born–Oppenheimer approximation), this becomes (with the obvious notation $X_n \equiv X(t)$ etc):

$$X_{n+1} = (1 + \xi - \Delta t^2 \omega^2) X_n - \xi X_{n-1}. \tag{A.1}$$

Writing $\alpha = \omega\Delta t$, this has the solution (except for $\alpha = 1 - \sqrt{\xi}$, which represents critical damping):

$$X_n = Pa_1^n + Qa_2^n \tag{A.2}$$

where a_1 and a_2 are the solutions to the indicial equation and are given by:

$$2a = (1 + \xi - \alpha^2) \pm [(1 - \alpha)^2 - \xi][(1 + \alpha)^2 - \xi]. \tag{A.3}$$

For $\alpha = 1 - \sqrt{\xi}$, the solution is $X_n = (P + Qn)a^n$.

Except in extremely unusual circumstances, the larger (in magnitude) of these solutions will dominate in the relaxation process. The dependence of the solutions on α (and hence on the time step) is outlined here.

For small α, the larger root is approximately $1 - \alpha^2(1 - \xi)$, so convergence is improved by reducing the applied damping. This root becomes smaller, and the other root increases, until they meet at the critical damping point $\alpha = 1 - \sqrt{\xi}$, when $a = \sqrt{\xi}$. For $1 - \sqrt{\xi} < \alpha < 1 + \sqrt{\xi}$, the roots are complex conjugates, with constant magnitude $\sqrt{\xi}$ and phase moving from 0 to $\pm\pi$ (so the mode will decay in some oscillatory fashion, as a real linear combination of these two solutions). At $\alpha = 1 + \sqrt{\xi}$, the roots become real again, this time both negative, and as α becomes large, the larger root (in magnitude) tends to $1 + \xi - \alpha^2$. There are no stationary values of a. The absolute upper limit of α for which relaxation can take place is $[2(1 + \xi)]^{1/2}$, above which $a < -1$; this is the only possible means by which instability can be generated.

A graph of $|a|$ against α, plotted for a range of damping factors in figure A1, shows how an increase in ξ reduces the maximum speed of relaxation, but increases the range of frequencies over which relaxation can effectively take place. Finding optimal values of ξ and Δt therefore involves a trade-off between these two considerations; what is important is the frequency range over which we expect to observe (and hence to have to 'freeze out') normal modes.

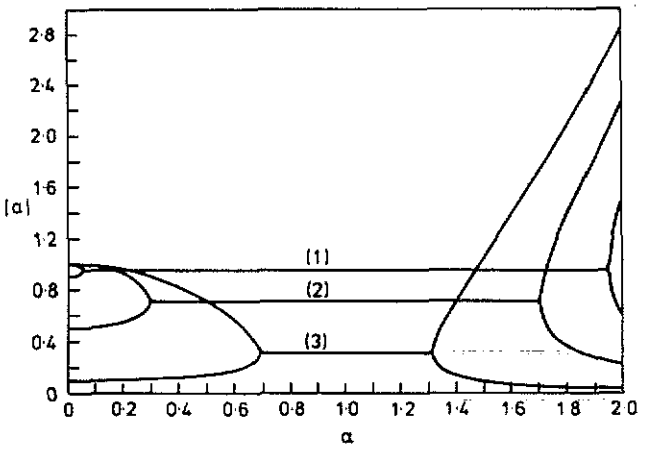

Figure A1. Magnitude of the roots, a_1 and a_2, of the indicial equation, which govern the rate of decay of normal mode amplitude, plotted against effective time step $\alpha = \omega\Delta t$. The damping parameters are (1) $\xi = 0.9$, (2) $\xi = 0.5$ and (3) $\xi = 0.1$.

If we expect modes with angular velocities between ω_{min} and $\omega_{max}(= R\omega_{min})$, we can obtain minimization at constant speed by choosing $\xi = [(R-1)/(R+1)]^2$, $\Delta t = 2(\omega_{min} + \omega_{max})$; the amount of each normal mode will be reduced by a factor $\sqrt{\xi}$ at each step.

A typical range of frequencies that we may need to consider might be the range $500\,cm^{-1}$ to $5000\,cm^{-1}$ (recall that values calculated by CNDO tend to be 50–60% higher than experimentally observed, so the C–H bond stretch typically observed at around 3300 cm^{-1} should occur at about $5000\,cm^{-1}$ in CNDO; stretching modes involving hydrogen will normally be the highest frequency modes that need be considered. The natural units of the calculation are such that $\omega = 1$ represents a frequency of approximately 5120 cm^{-1}, so to optimize the speed of convergence throughout this range we could choose $\xi = 0.65$, $\Delta t = 1.8$. In this case the amount of each normal mode present should decay by about 20% on each step, corresponding to a requirement of about ten steps for each extra significant figure required in the relaxed geometry. It will be safer, if in doubt about the range of frequencies to be considered, to overdamp the system (with, say, $\xi = 0.5$, $\Delta t = 1.0$) than to underdamp it, the more so because of the non-linearity that may be encountered at large distortions and the possibility of violating the Born–Oppenheimer approximation; overdamping can never lead to instability, while underdamping can.

The advantages of a careful choice of ξ and Δt can be seen if we consider the geometry optimization of methane. We start (for the sake of this example) from an asymmetric state, where the initial modes present are essentially the H–C–H bend observed at 1306 cm^{-1} and the C–H symmetric stretch observed at 2914 cm^{-1} (Herzberg 1945). Consider three pairs of damping parameters: $\xi = 0$, $\Delta t = 1$ (designed to 'freeze out' the C–H mode as quickly as possible, with no regard to the bending mode), $\xi = 0.25$, $\Delta t = 1.5$ (designed to optimize convergence for $\omega \approx 0.3$–1.0, i.e. specifically chosen for this molecule) and $\xi = 0.65$, $\Delta t = 1.8$ (the all-purpose values above). The behaviours of a typical C–H bond length and one of the distorted H–C–H bond angles are shown in figures A2 and A3, respectively: the first pair, as predicted, finds the equilibrium bond length very quickly indeed, but convergence is slow as far as the angle is concerned; the all-purpose pair leads to moderately good convergence for both, but the pair chosen specifically for methane is the best of the three, converging well within ten steps or so (the atoms were held fixed for three steps, to allow the Fock matrix time to reach a reasonable approximation).

Appendix 2. Errors in forces and energy conservation

There are two principal sources of error in the molecular dynamics we describe, although neither of them has a significant effect in the calculations presented in this or the following paper. First, there are those that arise entirely from the finite time-step used in the integration of the ionic equations of motion, and which would be present even if we used a simple empirical inter-atomic potential function with no reference to the electrons. Typically, we have found that these errors introduce a high-frequency ripple in the total energy. Second, the Born–Oppenheimer approximation assumes that the motion of the nuclei is determined by the ground-state total energy surface of the electron system. This energy surface defines a conservative dynamics. In a method such as ours, the ground-state wavefunction is determined only approximately at each step. The Hellman–Feynman forces at each step therefore contain errors reflecting the

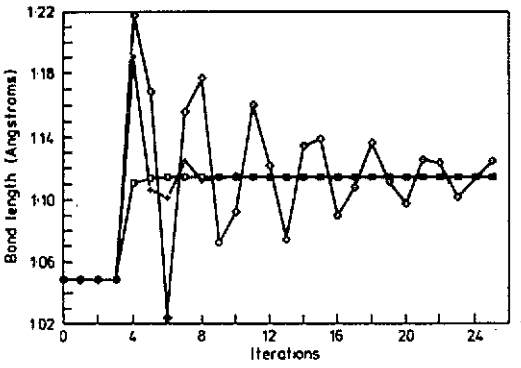

Figure A2. Change in the C–H bond length of methane throughout a relaxation run. Parameters used: □ : $\xi = 0, \Delta t = 1$; + : $\xi = 0.25, \Delta t = 1.5$; ◇ : $\xi = 0.65, \Delta t = 1.5$.

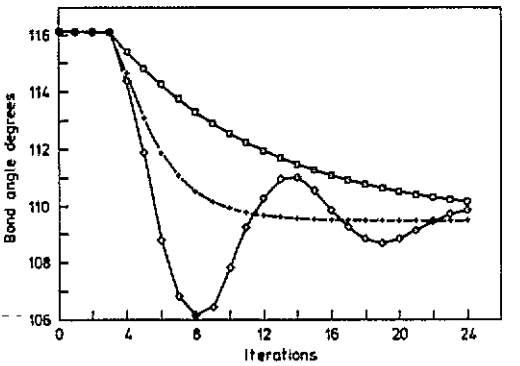

Figure A3. Change in the H–C–H bond angle of methane throughout a relaxation run. Parameters used: □ : $\xi = 0, \Delta t = 1$; + : $\xi = 0.25, \Delta t = 1.5$; ◇ : $\xi = 0.65, \Delta t = 1.5$.

errors in the wavefunctions and the potential surface for the nuclei is not a single-valued function of position. We find that this type of error introduces a long-term damping of the atomic dynamics as energy is transferred from the ions to the electrons.

For calculations in which we wish to damp the atomic dynamics and use it simply as a search procedure for the minimum-energy geometry of the system, these errors are of no significance. The system will relax to a position where the Hellman–Feynman forces are self-consistently zero, regardless of any errors made along the way. This point has been stressed by Gillan (1989). However, if we are to perform undamped molecular dynamics in simulation of the actual evolution of the system, we must be sure that the errors are not significant. We can quantify the errors of the first type by examining the effect of using improved algorithms for the integration of the ionic equations of motion so that the error is of higher order in the time step. The second type of error can be quantified by examining the effect of increasing the number of diagonalizations of the Fock matrix performed at each time step. Larger numbers of diagonalizations will bring the electron system nearer to self-consistency at each stage, and the dynamics will approach the results which would be obtained if we had performed a fully self-consistent calculation at each step.

To illustrate these points, we show in figure A4 the total (kinetic plus potential) energy as a function of time step for some test calculations performed without damping on the formaldehyde molecule, CH_2O. In figure A4(a), performed with a time step of 1.00 unit and with one diagonalization of the Fock matrix, the total energy has only a small ripple despite large oscillations in the internal and kinetic energies separately (not shown). In addition, there is a decay of the motion with a time constant of several tens of steps.

This steady decay reflects the damping of the dynamics that arises because the electronic system is not in its ground state and the dynamics is not conservative. This can be seen if we increase the number of diagonalizations of the Fock matrix per step to four, obtaining the results shown in figure A4(b). While the high-frequency oscillations in the energy are almost unchanged, the time constant for the decay of the motion has increased. Figure A4(c) shows a similar calculation in which the lower-order velocity

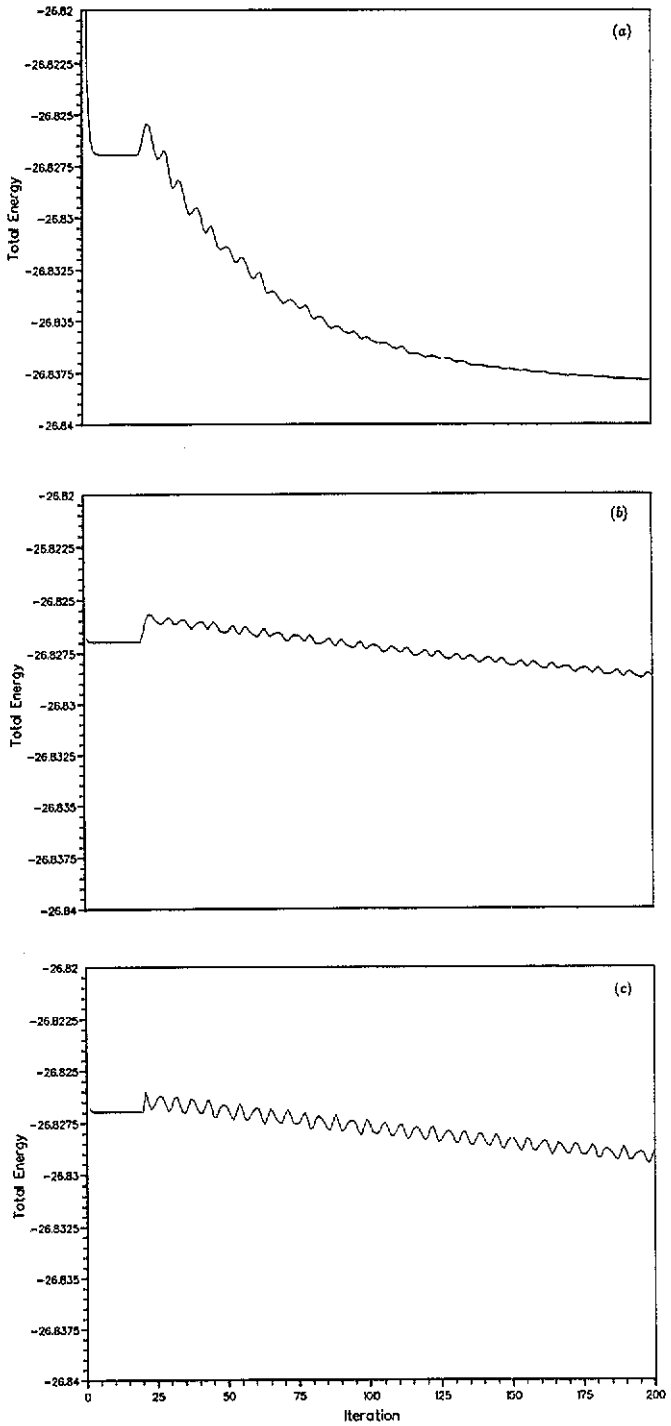

Figure A4. Variation of the total (kinetic plus potential) energy with time for formaldehyde with a timestep of 1.0 unit: (*a*) one diagonalization of the Fock matrix per tim step using the Beeman algorithm to update the atomic positions; (*b*) four diagonalizations per time step; (*c*) four diagonalizations per time step using the velocity Verlet algorithm for updating the atomic positions.

Verlet algorithm (Swope *et al* 1982) has been used instead of Beeman's algorithm to integrate the ionic equations of motion; here we see that the time constant is the same but that the high-frequency ripple in the energy has increased.

It is of some interest to compare these results with those that have been reported using the original Car–Parrinello method in which molecular dynamics is used to evolve the electronic as well as the ionic degrees of freedom. In that case, for a 16 atom system, fluctuations in the total (kinetic plus potential) energy of the ions are observed at a level of about 10^{-4} a.u. with a timestep of 1.7×10^{-16}s. In figure A5 we display the total energy for a calculation using the present program with a similar timestep. The short-period fluctuations in the total energy are similar but the overall decay is more rapid. This reflects the fact that the use of second-order equations of motion is particularly effective in limiting the rate of energy transfer between the ionic and electronic systems (Payne 1989). However, none of our conclusions, in this paper or the next, are affected by this small damping over large timescales.

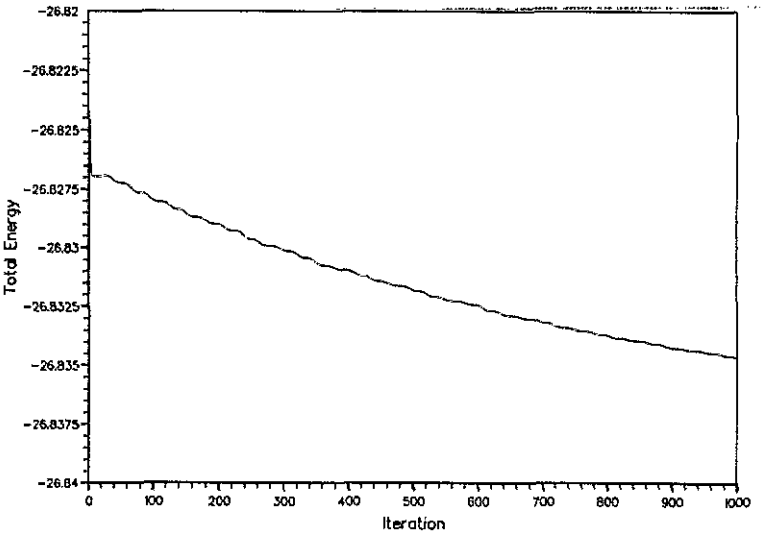

Figure A5. Total energy of the formaldehyde molecule as a function of time with a timestep of 1.0 unit and one diagonalization per time step.

References

Allinger N L 1976 *Adv. Phys. Org. Chem.* **13** 1
Beeman D 1976 *J. Comp. Phys.* **20** 130
Car R and Parrinello M 1985 *Phys. Rev. Lett.* **55** 2471
—— 1988 *Phys. Rev. Lett.* **60** 204
Davies D W 1969 *Mol. Phys.* **17** 473
Denbigh K G 1940 *Trans. Faraday Soc.* **36** 936
Galli G, Martin R W, Car R and Parrinello M 1989 *Phys. Rev. Lett.* **62** 555
Gillan M J 1989 *J. Phys.: Condens. Matter* **1** 689
Herzberg G 1945 *Molecular Spectra and Molecular Structure* vol. 2 (Princeton, NJ: van Nostrand)
Ivash E V and Dennison D M 1953 *J. Chem . Phys.* **21** 1804
Kolker H J and Karplus M 1963 *J. Chem. Phys.* **39** 2011
Landolt H and Börnstein 1951 *Zahlenwerte und Functionen* (Berlin: Springer)

McIver J W and Komornicki A 1971 *Chem. Phys. Lett.* **10** 303
Mori Y and Kurihara S 1988 *Synth. Met.* **24** 357
Needels M, Payne M C and Joannopoulos J D 1987 *Phys. Rev. Lett.* **58** 1765
Parr R G 1952 *J. Chem. Phys.* **20** 1499
Payne M C 1989 *J. Phys.: Condens. Matter* **1** 2199
Payne M C, Bristowe P D and Joannopoulos J D 1987 *Phys. Rev. Lett.* **58** 1348
Pulay P 1969 *Mol. Phys.* **17** 197
Pulay P and Török F 1973 *Mol. Phys.* **25** 1153
Pople J A and Beveridge D L 1970 *Approximate Molecular Orbital Theory* (New York: McGraw-Hill)
Pople J A and Gordon M S 1967 *J. Am. Chem. Soc.* **89** 4253
Powell M J D 1964 *Computer J.* **7** 155
Ramos M M D, Stoneham A M, Sutton A P and Pethica J B 1990 *J. Phys.: Condens. Matter* **2** 5913
Ryckaert J P, Cicotti G and Berendsen H J C 1977 *J. Comp. Phys.* **23** 327
Sadlej J 1985 *Semi-Empirical Methods in Quantum Chemistry* (Chichester: Ellis Horwood)
Slater J C 1974 *Quantum Theory of Molecules and Solids* vol. 4 (New York: McGraw-Hill)
Stevens R M and Lipscomb W N 1964 *J. Chem. Phys.* **41** 184
Stoneham A M 1989 *J. Computer-Aided Mol. Design* **3** 355
Stoneham A M and Bartram R H 1970 *Phys. Rev.* B **2** 3403
Swope W C, Andersen H C, Berens P H and Wilson K R 1982 *J. Chem. Phys.* **76** 637
Tarnow E, Joannopoulos J D and Payne M C 1989 *Phys. Rev.* B **39** 6017
Verlet L 1967 *Phys. Rev.* **159** 98
Wallace D S 1989 *D.Phil Thesis, University of Oxford and Harwell Laboratory Theoretical Physics Division Report* TP.1331